

Molecular Regulation of GLUT-4 Targeting in 3T3-L1 Adipocytes

Brad J. Marsh, Richard A. Alm, Shane R. McIntosh, and David E. James

Centre for Molecular and Cellular Biology, and the Department of Physiology and Pharmacology, The University of Queensland, St. Lucia, Q 4068, Australia

Abstract. Insulin stimulates glucose transport in muscle and adipose tissue by triggering the movement of the glucose transporter GLUT-4 from an intracellular compartment to the cell surface. Fundamental to this process is the intracellular sequestration of GLUT-4 in nonstimulated cells. Two distinct targeting motifs in the amino and carboxy termini of GLUT-4 have been previously identified by expressing chimeras comprised of portions of GLUT-4 and GLUT-1, a transporter isoform that is constitutively targeted to the cell surface, in heterologous cells. These motifs—FQQI in the NH₂ terminus and LL in the COOH terminus—resemble endocytic signals that have been described in other proteins. In the present study we have investigated the roles of these motifs in GLUT-4 targeting in insulin-sensitive cells. Epitope-tagged GLUT-4 constructs engineered to differentiate between endogenous and transfected GLUT-4 were stably expressed in 3T3-L1 adipocytes. Targeting was assessed in cells incubated in

the presence or absence of insulin by subcellular fractionation. The targeting of epitope-tagged GLUT-4 was indistinguishable from endogenous GLUT-4. Mutation of the FQQI motif (F⁵ to A⁵) caused GLUT-4 to constitutively accumulate at the cell surface regardless of expression level. Mutation of the dileucine motif (L⁴⁸⁹L⁴⁹⁰ to A⁴⁸⁹A⁴⁹⁰) caused an increase in cell surface distribution only at higher levels of expression, but the overall cell surface distribution of this mutant was less than that of the amino-terminal mutants. Both NH₂- and COOH-terminal mutants retained insulin-dependent movement from an intracellular to a cell surface locale, suggesting that neither of these motifs is involved in the insulin-dependent redistribution of GLUT-4. We conclude that the phenylalanine-based NH₂-terminal and the dileucine-based COOH-terminal motifs play important and distinct roles in GLUT-4 targeting in 3T3-L1 adipocytes.

THE mammalian facilitative glucose transporter family consists of six isoforms, referred to as GLUTs¹, which are highly homologous in both primary amino acid sequence and predicted secondary topology. Heterology between isoforms occurs mainly within the cytoplasmic amino and carboxy termini (Bell et al., 1990; reviewed in James et al., 1993). GLUT-4 is expressed exclusively in cardiac and skeletal muscle, and adipose tissue (James et al., 1988, 1989; Birnbaum, 1989; Charron et al., 1989; Fukumoto et al., 1989). Insulin stimulates the uptake of glucose in these tissues to maintain blood glucose ho-

meostasis under normal physiological conditions. This process is largely facilitated by the rapid translocation of GLUT-4 from an intracellular compartment to the plasma membrane in response to the binding of insulin to its cell surface receptor, and is associated with a 10–30-fold increase in glucose uptake (Cushman and Wardzala, 1980; Suzuki and Kono, 1980). Immunogold labeling and EM analysis of rat cardiac myocytes and adipocytes has shown that in the absence of insulin, GLUT-4 is sequestered predominantly within tubulo-vesicular structures clustered either in the *trans*-Golgi reticulum (TGR) or in the cytoplasm (Slot et al., 1991a,b). With insulin treatment, a marked increase in cell surface GLUT-4 labeling (~42% of the total) was observed with a corresponding decrease in labeling within intracellular structures (Slot et al., 1991a,b).

The intracellular sequestration of GLUT-4 is unique, as other isoforms, such as GLUT-1, have a high cell surface distribution in the absence of insulin (Calderhead et al., 1990; Piper et al., 1991; Haney et al., 1991; Hudson et al., 1992). GLUT-4 is sequestered within intracellular tubulo-vesicular structures when expressed in heterologous cell types such as fibroblasts, HepG2 hepatoma and CHO cells

In an accompanying manuscript, Verhey et al. also present the results of GLUT-4 targeting in 3T3-L1 adipocytes. This study reached similar conclusions to those found in our own study.

Address correspondence to David E. James, Centre for Molecular and Cellular Biology, The University of Queensland, St. Lucia, Q 4068, Australia. Tel.: 61 733654986. Fax: 61 733654388.

1. *Abbreviations used in this paper:* ECL, enhanced chemiluminescence; GLUT, glucose transporter protein isoform; HDM, high-density microsomes; KRP, Krebs-Ringer phosphate; LDM, low-density microsomes; M/N, mitochondria/nuclei; PM, plasma membrane; TGR, trans-Golgi reticulum.

(Haney et al., 1991; Asano et al., 1992; Hudson et al., 1992). However, the insulin-dependent movement of GLUT-4 to the cell surface is minimal in these cells (Haney et al., 1991; Robinson et al., 1992; Verhey et al., 1993). This strongly suggests that the subcellular targeting of these glucose transporters reflects their heterologous amino acid sequences and that factors that regulate their intracellular targeting are both shared by many cell types and separate from those factors that may be specific to muscle and adipose cells and that regulate insulin-dependent translocation to the plasma membrane.

In an attempt to define the relevant targeting domains that direct the intracellular sequestration of GLUT-4, chimeric studies have been performed in fibroblasts in which reciprocal domains were exchanged between GLUT-4 and GLUT-1. These studies identified functional domains in both the amino and carboxy termini, and in transmembrane regions 7 and 8 (Asano et al., 1992; Piper et al., 1992; Czech et al., 1993; Marshall et al., 1993; Verhey et al., 1993). Site-directed mutagenesis has revealed that phenylalanine at position 5 in GLUT-4 is a critical component of an NH₂-terminal targeting motif comprising residues 2–8 (PSGFQQI) that is “both necessary and sufficient for intracellular sequestration” when substituted onto the H1 subunit of the asialoglycoprotein receptor (Piper et al., 1993). A dileucine motif at positions 489 and 490 was additionally identified as a critical component of the COOH-terminal signal for both endocytosis and intracellular sequestration of GLUT-4 (Corvera et al., 1994; Verhey and Birnbaum, 1994).

A potential problem with the above studies is that they have been performed in cell types that are not considered to be bona-fide insulin-sensitive cells, and are therefore unlikely to contain the cell-specific factors that facilitate the insulin-regulated translocation of GLUT-4 to the plasma membrane. It has remained unclear whether these domains function to regulate GLUT-4 targeting in the context of an appropriate insulin-responsive cellular environment. In addition, contradictory reports between laboratories with respect to the targeting of analogous GLUT-1/GLUT-4 chimeras suggest that differences in the level of chimera expression may influence the resultant targeting of these proteins (reviewed in James and Piper, 1994).

To address these problems we have stably expressed GLUT-4 mutants in 3T3-L1 adipocytes, a cell type that exhibits insulin-regulatable glucose transport. Because these cells express GLUT-4, an epitope tag has been used to distinguish recombinant GLUT-4 from the endogenous GLUT-4. We show that the epitope-tagged GLUT-4 construct behaves indistinguishably from endogenous GLUT-4, and we further show that mutation of either phenylalanine⁵ in the NH₂-terminal or leucine⁴⁸⁹-leucine⁴⁹⁰ in the COOH-terminal domains results in impaired targeting of GLUT-4 in 3T3-L1 adipocytes.

Materials and Methods

Cell Culture

Murine fibroblasts obtained from the American Type Culture Collection (Rockville, MD) were cultured in DME containing high glucose, L-gluta-

mine and sodium pyruvate supplemented with 10% bovine calf serum (CSL, Parkville, Australia). Cells were maintained and passaged as pre-confluent cultures at 37°C in a 5% CO₂ humidified incubator before differentiation. All experiments utilized adipocytes 10–14 d after initiation of differentiation. 3T3-L1 fibroblasts were induced to differentiate 3 d after reaching confluence by the addition of DME containing 5% heat-inactivated FCS (CSL), 4 μg/ml insulin, 0.25 mM dexamethasone, 0.5 mM 3-isobutyl-1-methylxanthine and 100 ng/ml d-biotin. After 72 h, induction medium was replaced with fresh FCS/DME containing 4 μg/ml insulin and 100 ng/ml d-biotin.

Construction of Human GLUT-3 Epitope-tagged Transporter cDNAs

Wild-type rat GLUT-4 cDNA cloned into pBluescript (pIRGT) (Piper et al., 1993) was epitope-tagged at the COOH terminus by the addition of amino acids 485–496 from human GLUT-3. This construct was generated by PCR using the vector T7 primer and an oligonucleotide encompassing a XhoI restriction site, the GLUT-3 sequence and the overlapping sequence of the GLUT-4 cDNA. The PCR conditions used were identical to those described previously (Piper et al., 1993). The PCR product containing the GLUT-3 epitope was digested with BglII-XhoI, and the ~140 bp fragment was subcloned into the BglII-XhoI sites of pIRGT to generate pTAG. The pFAG construct was generated by removing the XbaI-SacII fragment containing the NH₂ terminus from the F⁵ to A⁵ mutant described previously (Piper et al., 1993) and ligating into the pTAG backbone. The L⁴⁸⁹L⁴⁹⁰ to A⁴⁸⁹A⁴⁹⁰ mutant in pIRGT was constructed using a PCR technique described previously (Alm and Mattick, 1995). This mutant was then used as the template DNA in a PCR reaction identical to that employed to generate the pTAG construct. Finally, the COOH terminus containing the GLUT-3 epitope and the L⁴⁸⁹L⁴⁹⁰ to A⁴⁸⁹A⁴⁹⁰ mutation were subcloned into the BglII-XhoI sites of pIRGT to generate pLAG. All regions of the cDNA constructs produced by PCR were entirely sequenced.

To facilitate insertion of these cDNA constructs into the pMEXneo expression vector (kindly provided by Dr. E. Santos, National Institutes of Health, Bethesda, MD) (Benito et al., 1991) for stable transfection, they were all removed as XbaI-XhoI fragments into a shuttle vector that was essentially pBluescript with a modified multiple cloning site region such that the XbaI and XhoI restriction sites were flanked by BamHI and KpnI restriction sites, respectively. Once subcloned into this shuttle vector, the cDNA constructs could be removed as BamHI-KpnI fragments and then inserted directionally into the pMEXneo vector under the control of the MSV-LTR promoter.

Stable Transfection of cDNA Transporter Constructs into 3T3-L1 Fibroblasts

Recombinant GLUT-4 cDNA constructs subcloned into the BamHI and KpnI sites of the mammalian expression vector pMEXneo were transfected into subconfluent 3T3-L1 fibroblasts using the Lipofectamine reagent, according to the manufacturer's protocol (GIBCO BRL, Gaithersburg, MD). Individual neomycin-resistant colonies were selected in media containing 0.8 mg/ml G418 (GIBCO BRL) and isolated using glass cloning rings. Clones were screened as follows.

Immunofluorescence microscopy. To assess clonality of expression, fibroblasts cultured on ethanol-washed glass coverslips were fixed in 2% paraformaldehyde, permeabilized, and immunolabeled with antibodies specific for either GLUT-4 or the human GLUT-3 epitope tag as described previously (Piper et al., 1991, 1992). Primary antibodies were detected with FITC-conjugated sheep anti-rabbit secondary antibody (25 μg/ml) (The Binding Site, Birmingham, UK). Coverslips were mounted on glass slides as previously described (Piper et al., 1991) and were visualized with a 63×/1.40 Zeiss oil immersion lens using a Zeiss Axioskop fluorescence microscope (Carl Zeiss, Germany) equipped with a Bio-Rad MRC-600 laser confocal imaging system. Images were collected directly using identical photomultiplier tube, numerical aperture and gain settings.

Differentiation. Fibroblasts were grown to confluence in 60-mm plates and induced to differentiate as described above. Clones in which >90% of fibroblasts successfully differentiated into mature adipocytes in culture were maintained and subjected to further analysis.

Immunoblotting of total cellular membranes. Fibroblasts or adipocytes cultured in 60-mm plates were scraped in Hepes buffer (20 mM, pH 7.4) containing 1 mM EDTA and 250 mM sucrose (HES), lysed using a 1-ml sy-

ringe and 27-gauge needle and centrifuged at 208,000 *g* for 30 min in a TLA-100.3 rotor (Beckman, Palo Alto, CA, USA) to pellet total cellular membranes. Membrane pellets were resuspended in 1% SDS in HES buffer and subjected to SDS-PAGE and immunoblotting using antibodies specific for either the COOH terminus of GLUT-4 or human GLUT-3. This procedure provided an assessment of the relative expression levels of each clone.

Subcellular Distribution of Transporter Constructs in 3T3-L1 Adipocytes

Two separate methods were employed to assess the subcellular distribution of recombinant GLUT-4 transporters in 3T3-L1 adipocytes.

Differential Centrifugation. Subcellular membrane fractions were prepared by differential centrifugation from transfected adipocytes in basal and insulin-stimulated states using a method described in detail previously (Piper et al., 1991). Briefly, adipocytes grown in 100-mm plates were washed three times with sterile, prewarmed PBS and incubated for 2 h at 37°C in 10 ml of Krebs-Ringer phosphate (KRP) buffer containing 2% BSA and 2.5 mM glucose. Cells were then further incubated for 30 min at 37°C in either KRP containing 4 µg/ml insulin (insulin-stimulated) or in KRP with no additions (basal) (2 × 100-mm plates were used per condition).

All subsequent steps were carried out at 0–4°C. The cells were washed three times with 5 ml HES buffer and scraped from the plate with a rubber policeman in HES containing PMSF (50 µg/ml) and aprotinin (10 µg/ml) (2 ml/plate). Cells were homogenized by 10–12 passages through a Balch homogenizer containing a stainless steel ball bearing (diameter 0.2510") (Balch et al., 1984). The homogenate was subjected to differential centrifugation using a previously described protocol (Piper et al., 1991) to generate four membrane fractions designated as high-density microsomes (HDM), low-density microsomes (LDM), plasma membranes (PM), and mitochondria/nuclei (M/N). Most of our studies were performed using the PM and LDM fractions because these fractions are enriched in cell surface membrane and membranes encompassing the intracellular GLUT-4 compartment, respectively (Piper et al., 1991). Membranes were resuspended in HES buffer and stored at –20°C. The protein yields for each of the four subcellular membrane fractions recovered from 3T3-L1 adipocytes by differential centrifugation were not significantly different from those described previously (Piper et al., 1991). Furthermore, we did not observe significant variance in these protein yields between individual clonal cell lines.

Plasma Membrane Lawn Assay. The subcellular distribution of recombinant transporters was also assessed by immunofluorescence labeling of plasma membrane fragments prepared from basal and insulin-stimulated adipocytes as described previously (Robinson and James, 1992; Robinson et al., 1992). Briefly, adipocytes were grown on glass coverslips and sonicated using a probe sonicator (Kontes, Vineland, NJ) to generate a lawn of PM fragments that remained attached to the glass. These fragments were then immunolabeled with either polyclonal antibodies specific for either GLUT-4 or the human GLUT-3 epitope-tag. Coverslips were visualized and imaged using a confocal laser scanning immunofluorescence microscope as described above.

Electrophoresis and Immunoblotting

Equivalent amounts of protein from total cellular membranes (20 µg) or subcellular membrane fractions (10 µg) were subjected to SDS-PAGE using 10 or 12% polyacrylamide resolving gels. Proteins were electrophoretically transferred to supported nitrocellulose membranes (Amersham, Little Chalfont, Buckinghamshire, UK) and immunoblotted with polyclonal antibodies specific for the COOH termini of GLUT-4 (R820), GLUT-1 (R493), and human GLUT-3 (R1697), respectively. The anti-peptide polyclonal antibodies specific for the COOH terminus of GLUT-1 (R493), GLUT-4 (R820) and the 12 carboxy-terminal residues of human GLUT-3 (R1697) have been characterized and described previously (James et al., 1989; Piper et al., 1991; Harris et al., 1992). R493 and R1697 were affinity-purified against peptide antigen covalently coupled to a Sulfolink Coupling Gel column according to the manufacturer's instructions (Pierce Chem. Co., Rockford, IL). Primary antibodies were detected by probing with HRP-conjugated donkey anti-rabbit secondary antibody diluted 1:10,000 and blots developed using the technique of enhanced chemiluminescence (ECL) according to the manufacturer's instructions (Amersham). Autoradiograms were quantitated using a Model GS-670 Imaging Densitometer (Bio-Rad Labs., Richmond, CA). The level of recombinant

GLUT-4 at the PM with insulin was nominally assigned a value of 1 in these studies to normalize between individual determinations and between recombinant constructs expressed by different clones.

Protein Assays

The protein concentrations of total cellular membranes and subcellular membrane fractions prepared as above were determined using the bicinchoninic acid assay (Pierce Chem. Co.) according to the manufacturer's instructions.

Results

Targeting of Epitope-tagged GLUT-4

The constructs analyzed in this study are summarized in Fig. 1. To assess the contribution of phenylalanine at position 5 or the leucine pair at positions 489 and 490 to GLUT-4 targeting in 3T3-L1 adipocytes, it was necessary to include a foreign epitope in the GLUT-4 cDNA. Rather than introduce a foreign sequence at an intervening location within GLUT-4, an epitope tag was introduced at the extreme carboxy terminus in an attempt to preserve the overall structure of the protein. This protein reacted with both monoclonal (1F8, data not shown) and polyclonal (R820) anti-GLUT-4 COOH-terminal antibodies, and could be uniquely distinguished from endogenous wild-type GLUT-4 with a polyclonal anti-human GLUT-3 antibody (R1697) (see below). Several criteria were used to show that the inclusion of this epitope did not disrupt the native targeting of GLUT-4. The targeting of the recombinant epitope-tagged GLUT-4 protein, referred to here as TAG, was indistinguishable from wild-type GLUT-4 expressed in 3T3-L1 fibroblasts by stable transfection (Haney et al., 1991). Confocal laser immunofluorescence microscopy of

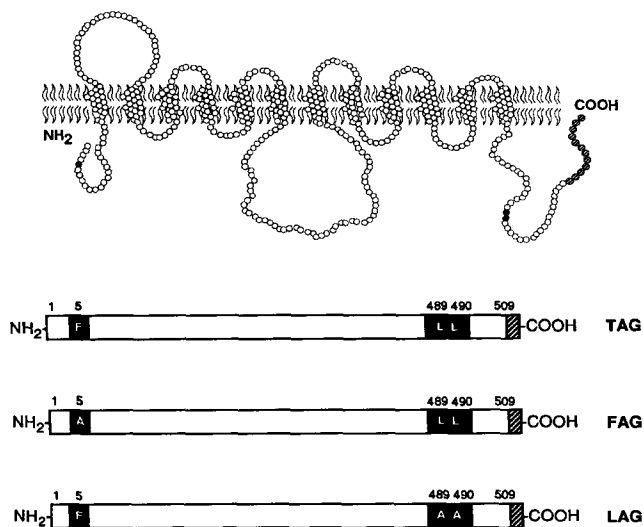


Figure 1. Summary of the recombinant GLUT-4 constructs used in these studies. A foreign epitope encompassing the carboxy-terminal 12-amino acid residues from human GLUT-3 (shaded) was engineered as an additional tag at the 3' end of the full-length GLUT-4 cDNA. The positions at which site-directed mutagenesis was performed are shown in black. Amino acid residues are represented using the single letter code.

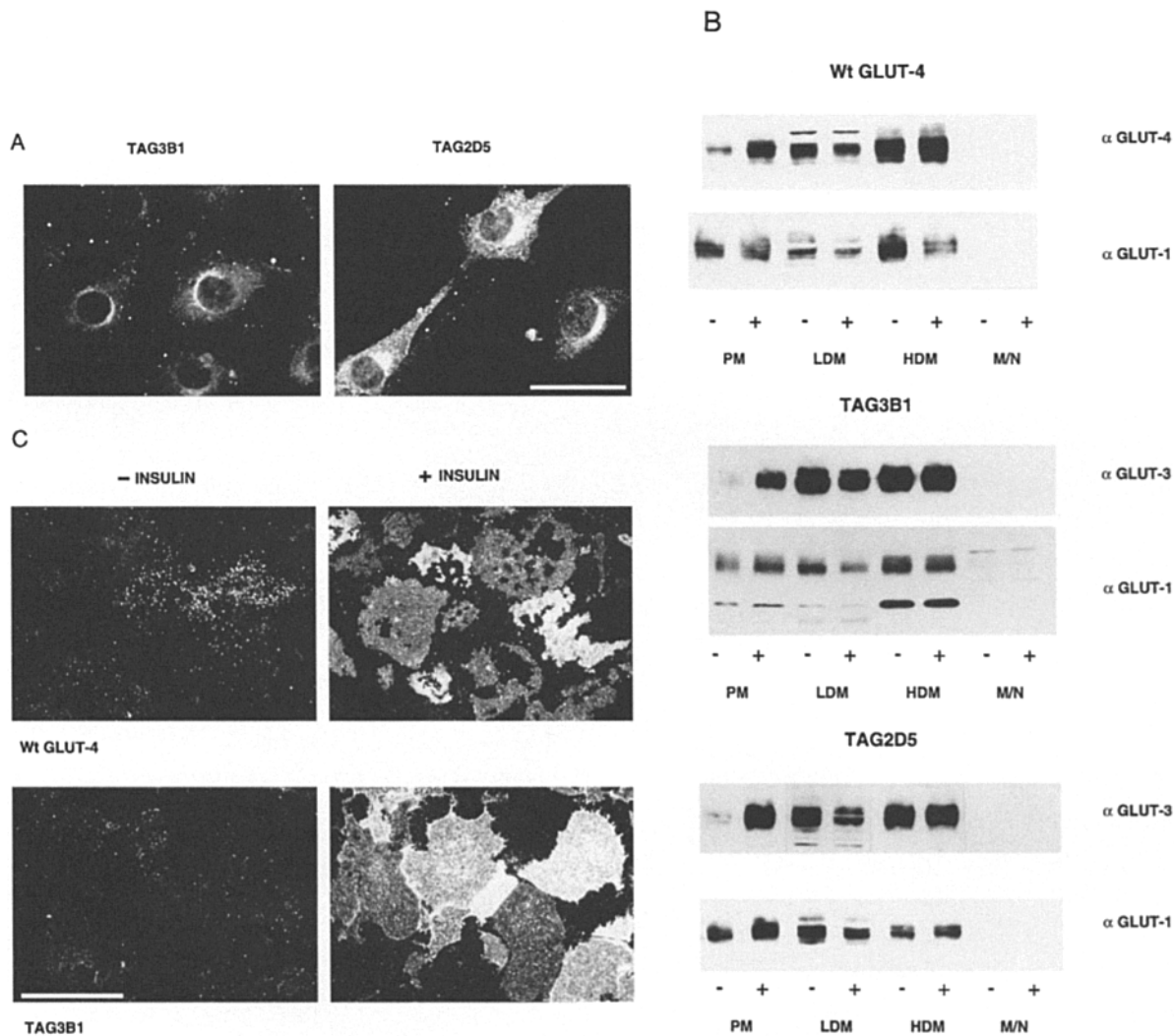


Figure 2. Localization of TAG in stably transfected 3T3-L1 cells. (A) Immunolocalization of TAG in stably-transfected 3T3-L1 fibroblasts by confocal immunofluorescence microscopy. Cells were fixed, permeabilized, and labeled with an antibody specific for the COOH terminus of GLUT-4 (R820) and FITC-conjugated sheep anti-rabbit antibody. Shown are fibroblast clones TAG3B1 (*left*) and TAG2D5 (*right*). Images were collected, adjusted for brightness and contrast and printed using identical conditions. (B and C) Subcellular distribution of wild-type GLUT-4 and epitope-tagged recombinant GLUT-4 (TAG) in basal (–) and insulin-stimulated (+) 3T3-L1 adipocytes. In B, subcellular membrane fractions (10 μ g) were prepared by differential centrifugation and subjected to SDS-PAGE, electrophoretically transferred to nitrocellulose membranes and immunoblotted with antibodies specific for the COOH terminus of GLUT-4 (R820), the COOH terminus of GLUT-1 (R493), or for the human GLUT-3 epitope tag (R1697). Signals were detected by enhanced chemiluminescence (ECL). (C) Immunofluorescence labeling of PM lawns prepared from naive (*top*) or TAG-transfected (*bottom*) 3T3-L1 adipocytes incubated in the absence (*left*) or presence (*right*) of insulin for 15 min at 37°C. Plasma membrane fragments prepared from untransfected or TAG-transfected adipocytes were immunolabeled with either GLUT-4- or human GLUT-3-specific antibodies, respectively. Bars, 50 μ m.

fibroblasts (Fig. 2 A) and immuno-EM of adipocytes (data not shown) revealed that TAG was localized to tubulovesicular elements that were either clustered in the TGR or in the cytoplasm.

Moreover, the targeting of TAG was indistinguishable from endogenous GLUT-4 in 3T3-L1 adipocytes. In the absence of insulin, TAG was excluded from the PM fraction and was located predominantly within a vesicle population designated LDM fraction (Fig. 2 B), which has previously been shown to be enriched in the intracellular GLUT-4 compartment in adipocytes (Simpson et al., 1983; Piper et al., 1991). Insulin treatment resulted in a significant increase in TAG levels in the PM fraction, with a cor-

responding decrease in the levels of TAG in the intracellular LDM. A more accurate assessment of the magnitude of the insulin-dependent movement of both TAG and endogenous GLUT-4 to the cell surface was obtained using the PM lawn assay (Fig. 2 C). This procedure generates highly purified PM fragments attached to glass coverslips (Robinson et al., 1992) and provides a more sensitive index of insulin action. PM fragments isolated from basal cells exhibited very low levels of either TAG or endogenous GLUT-4 labeling (Fig. 2 C, *left*). A 5–10-fold increase in labeling for TAG and GLUT-4 was evident in PM fragments prepared from insulin-treated adipocytes (Fig. 2 C, *right*).

The distribution of TAG was similar in different clonal cell lines despite marked differences in TAG expression levels between different clones (see below). As an internal control for the integrity of the differential centrifugation procedure, all fractions were routinely immunoblotted with an anti-GLUT-1 antibody. Consistent with previous studies (Calderhead et al., 1990; Piper et al., 1991), GLUT-1 had a high cell surface distribution in comparison to either TAG or endogenous GLUT-4 in the absence of insulin (Fig. 2 B).

Expression of GLUT-4 Targeting Mutants in 3T3-L1 Cells

Clones were selected for further study based upon the level of recombinant protein expressed and their ability to undergo differentiation from fibroblasts into adipocytes following transfection (Fig. 3). Total cellular membranes from each clone were immunoblotted with an antibody specific for the GLUT-4 carboxy terminus to quantify the total level of recombinant transporter plus endogenous GLUT-4 expressed (Fig. 3, top). Clones were classified into two broad categories: low expressors, in which total GLUT-4 expression was at a level comparable to that of endogenous GLUT-4 in untransfected adipocytes, and high expressors, where total expression was greater than fourfold higher than for wild-type GLUT-4 expressed by 3T3-L1 adipocytes. To quantify relative expression of the recombinant transporters independently of endogenous GLUT-4, total cellular membranes were immunoblotted with the human GLUT-3 antibody (Fig. 3, bottom).

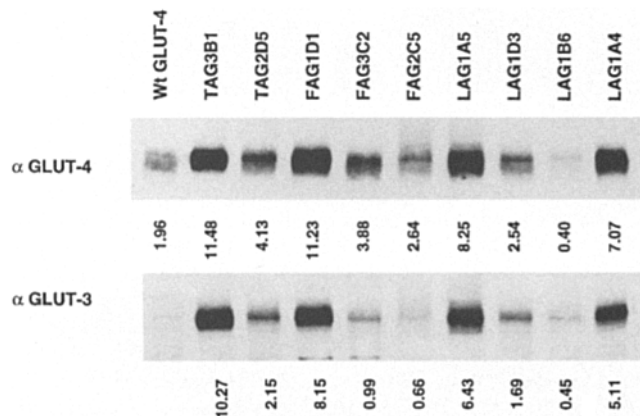


Figure 3. Relative expression levels of transfected GLUT-4 constructs in 3T3-L1 adipocyte clones. Total cellular membranes were isolated from individual 3T3-L1 cell lines. Samples (20 μ g of membrane protein) prepared from each clone were subjected to SDS-PAGE and immunoblotted using antibodies specific for COOH terminus of GLUT-4 (R820, top) or the human GLUT-3 epitope-tag (R1697, bottom). Autoradiograms were quantitated by densitometry and the results expressed as arbitrary units to assess the relative levels of endogenous plus transfected GLUT-4 and exogenous transporter alone expressed by each clone. Clones were classified into two broad categories based upon the total level of GLUT-4 expression relative to endogenous GLUT-4 expressed by wild-type 3T3-L1 adipocytes. High expressor clones included TAG3B1, FAG1D1, and LAG1A5. Adipocyte clones TAG2D5, FAG3C2, FAG2C5, LAG1D3, LAG1B6, and LAG1A4 were classified as low expressors.

In the case of TAG, its intracellular sequestration in the absence of insulin was maintained, irrespective of expression level. Despite a fourfold difference in expression level between TAG clones 3B1 and 2D5, the intracellular sequestration of TAG in both of these clonal cell lines was similar to that observed for wild-type GLUT-4. In the absence of insulin stimulation, PM fragments isolated from both TAG clone adipocytes exhibited low levels of labeling similar to that observed for wild-type GLUT-4 (Fig. 2 C). Furthermore, the effect of insulin on the subcellular distribution of TAG was similar over this range of expression (Fig. 4). However, it is noteworthy that the labeling of PM fragments isolated from clone TAG2D5 adipocytes cultured in the presence of insulin was significantly lower than for insulin-treated TAG3B1 PM fragments (not shown).

Targeting of the Phe to Ala Mutant (FAG) in Adipocytes

In agreement with previous studies (Piper et al., 1993), mutation of F⁵ to A⁵ within the amino terminus of epitope-tagged GLUT-4 (FAG) resulted in a marked increase in cell surface accumulation of the transporter. In 3T3-L1 fibroblasts, an increase in cell surface staining was apparent for clone FAG1D1 (not shown) and FAG3C2 fibroblasts compared to cell lines expressing TAG as determined by confocal immunofluorescence microscopy (Fig. 5 A). FAG was also immunolocalized to a perinuclear region similar to that observed for TAG in 3T3-L1 fibroblasts (Fig. 5 A). Despite a level of expression only marginally lower than FAG3C2, we were unable to visualize cell surface labeling of FAG2C5 fibroblasts using immunofluorescence microscopy. However, as previously described by Griffiths et al. (1993), this may reflect an artifact of this technique that arises because low labeling of diffuse surfaces such as the plasma membrane is much more difficult to detect than low but concentrated labeling of intracellular organelles.

The subcellular distribution of FAG and GLUT-1 was assessed by immunoblotting subcellular membrane fractions prepared from the differentiated cell lines with anti-

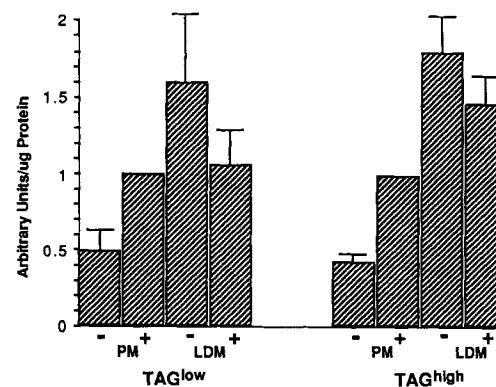


Figure 4. Subcellular distribution of epitope-tagged recombinant GLUT-4 (TAG) expressed at low (TAG2D5) or high (TAG3B1) levels in basal (-) and insulin-stimulated (+) 3T3-L1 adipocytes. The combined results of multiple independent differential centrifugation experiments immunoblotted with an antibody to the human GLUT-3 epitope tag and quantitated by densitometry were plotted for basal (-) and insulin-stimulated (+) adipocytes. Values are the means \pm SEM (arbitrary units/ μ g protein).

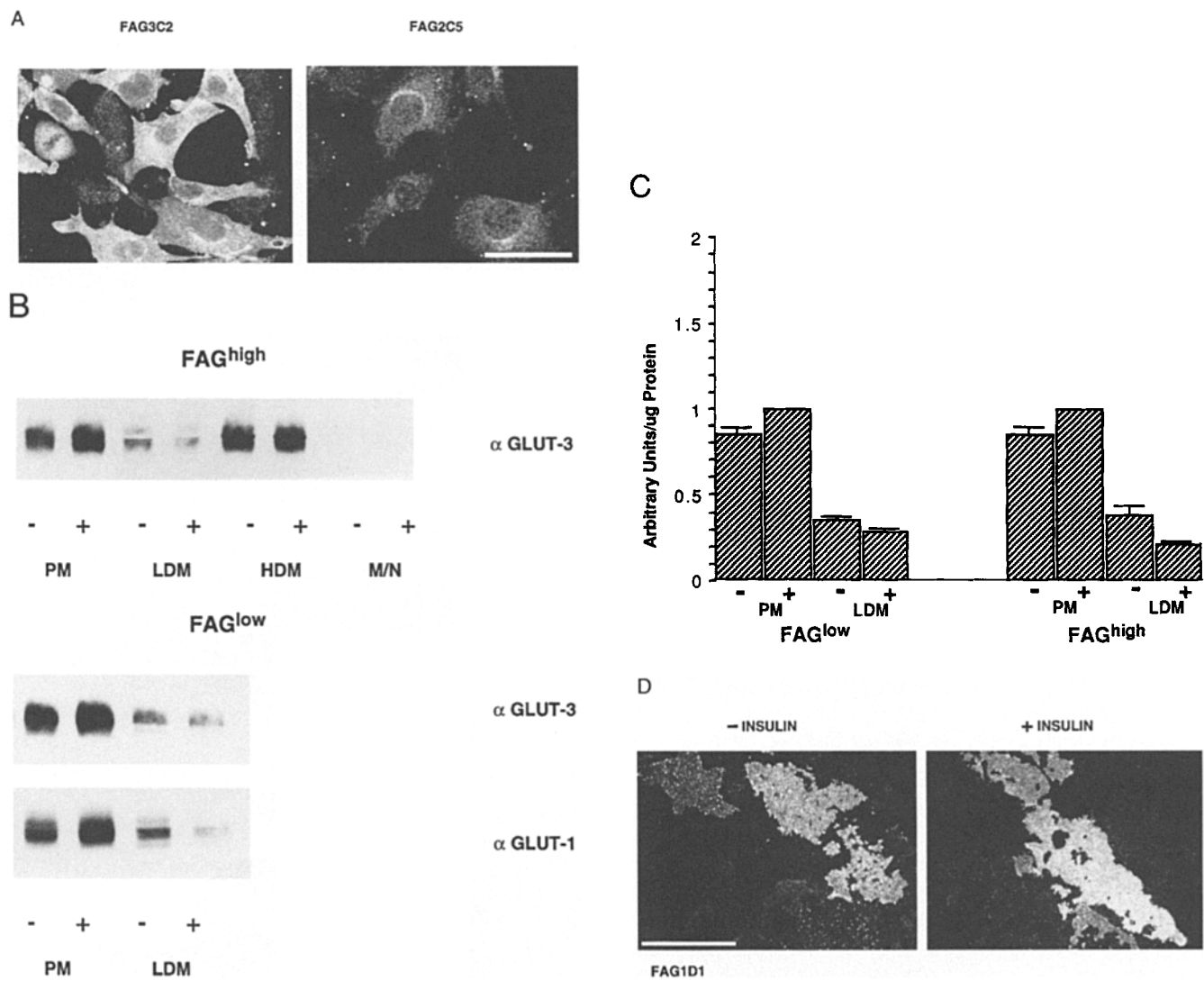


Figure 5. Localization of FAG in stably transfected 3T3-L1 cells. (A) Immunolocalization of FAG in stably transfected 3T3-L1 fibroblasts by confocal immunofluorescence microscopy. Cells were fixed, permeabilized, and labeled with an antibody specific for the COOH terminus of GLUT-4 (R820) and FITC-conjugated sheep anti-rabbit antibody. Shown are fibroblast clones FAG3C2 (left) and FAG2C5 (right). Images were collected, adjusted for brightness and contrast and printed using identical conditions. (B–D): Subcellular distribution of epitope-tagged recombinant GLUT-4 (FAG) expressed at high (FAG1D1) or low (FAG3C2 and FAG2C5) levels in basal (–) and insulin-stimulated (+) 3T3-L1 adipocytes. (B) Subcellular membrane fractions (10 μ g) prepared by differential centrifugation were subjected to SDS-PAGE, electrophoretically transferred to nitrocellulose membranes and immunoblotted with either an affinity-purified antibody specific for the human GLUT-3 epitope tag (R1697, top) or an antibody specific for the COOH terminus of GLUT-1 (R493, bottom). Signals were detected by ECL. (C) The combined results of multiple independent differential centrifugation experiments were quantitated by densitometry and plotted for basal (–) and insulin-stimulated (+) adipocytes. Values are the means \pm SEM (arbitrary units/ μ g protein). (D) Immunofluorescence labeling of PM lawns prepared from FAG-transfected 3T3-L1 adipocytes incubated in the absence (left) or presence (right) of insulin for 15 min at 37°C. Plasma membrane fragments prepared from FAG-transfected adipocytes were immunolabeled with the human GLUT-3 antibody. Bars: (A and D) 50 μ m.

bodies specific for the human GLUT-3 epitope tag (top), or GLUT-1 (bottom) (Fig. 5 B). Irrespective of the cell line or the expression level of recombinant protein examined, FAG exhibited a substantial targeting defect in adipocytes. Both differential centrifugation (Fig. 5 B) and immunolabeling of PM lawns (Fig. 5 D) revealed a marked accumulation of FAG in plasma membranes isolated from non-insulin-stimulated cells. The difference in the subcellular distribution of FAG and TAG is clearly demonstrated by comparing the PM/LDM ratio for each protein, which provides an index of the intracellular sequestration

of transporters (see Fig. 7). This ratio was extremely low for TAG (0.33 ± 0.09), reflecting a high degree of intracellular sequestration. In contrast, the PM/LDM ratio was seven- to eightfold higher for FAG (2.46 ± 0.38), reflecting the high level of FAG at the plasma membrane in comparison to the intracellular vesicle pool. It is noteworthy that the subcellular distribution of GLUT-1 in FAG-expressing clones was not significantly different from that seen in TAG-expressing clones, providing a useful internal control for the differential centrifugation procedure.

Despite the accumulation of FAG at the cell surface,

FAG mutants still exhibited a small insulin-dependent movement out of the LDM and to the plasma membrane fractions, although this was much less than observed for either TAG or wild-type GLUT-4 (Figs. 5, B and C). No visible staining of plasma membrane fragments in PM lawns prepared from either FAG3C2 or FAG2C5 was observed with the antibody specific for the epitope tag, due to the low levels of recombinant protein expressed by these clones.

Targeting of the Dileucine Mutant (LAG) in Adipocytes

Four clonal cell lines expressing LAG were isolated and used for subsequent study. These clones were selected based upon the level of LAG expression, which varied over a similar range to that observed in the TAG and FAG clones (see Fig. 3). In addition, the differentiation efficiency of these clones was very high as determined by the high percentage (>90%) of cells that exhibited multiple lipid droplets at >4 d after differentiation. In the undifferentiated state, high cell surface staining was clearly evident in the LAG clone (LAG1A4) by immunofluorescence microscopy (Fig. 6 A). However, as was the case for the lower expressing FAG clones, little if any detectable cell surface staining was evident in low expressing LAG fibroblasts (LAG1B6) (Fig. 6 A). All stably-transfected LAG-expressing fibroblasts exhibited a perinuclear pattern of staining similar to the pattern described for TAG and FAG (Fig. 6 A).

To further define the targeting of the dileucine mutant extensive experimentation was performed following differentiation of each of the clones into adipocytes. The subcellular distribution of LAG and GLUT-1 in a high expressing LAG adipocyte clone (LAG1A5, i.e., LAG^{high}), and in two adipocyte clones exhibiting low levels of expression (LAG1D3 and LAG1B6, i.e., LAG^{low}) are shown in Fig. 6 B. The two distinct subcellular fractionation techniques, that of differential centrifugation (Fig. 6 B) and labeling of PM lawns (Fig. 6 D), demonstrated that at low expression levels LAG was segregated between the intracellular compartment and the plasma membrane, in unstimulated adipocytes, to the same extent as TAG or wild-type GLUT-4 (Fig. 2, B and C). In contrast, LAG accumulated at the plasma membrane in the absence of insulin in clone LAG1A5, in which the expression of LAG was higher than in any of the other three LAG clones studied. This targeting difference is most clearly evident by comparing the PM/LDM ratios that were quantified based on fractionation of non-insulin-stimulated cells. In the case of the low expressors (LAG1D3 and LAG1B6) the combined ratio (0.32 ± 0.06) was not significantly different compared to TAG (0.33 ± 0.09). The ratio was significantly higher, however, in clone LAG1A5 (1.34 ± 0.17), indicating the high cell surface expression of LAG expressed by this clone. In addition, the PM/LDM ratio for LAG1A5 is not dissimilar to the ratio observed for GLUT-1 (1.26 ± 0.08). These data confirmed the staining patterns visualized in PM lawns prepared from basal adipocyte clones with either low-moderate (LAG1A4) or high (LAG1A5) levels of expression (Fig. 6 D).

The distribution of LAG in adipocyte clones expressing LAG at lower levels (LAG1D3 and LAG1B6) following insulin stimulation was indistinguishable from TAG or

wild-type GLUT-4 (Fig. 6, B and C). In both cases there was a significant shift in the distribution of LAG from the LDM fraction to the plasma membrane. Whereas there was an accumulation of LAG at the cell surface in clone LAG1A5 in the absence of insulin, there was still a significant movement of LAG from the LDM to the PM. However, in view of the high cell surface distribution of LAG in this clone in the basal state, the net magnitude of the insulin effect at the PM was reduced. The insulin-stimulated increase in labeling observed in PM fragments isolated from clone LAG1A4 (Fig. 6 D, bottom right) was not significantly different from either wild-type GLUT-4 or TAG. PM lawns isolated from clones LAG1D3 and LAG1B6 and immunolabeled with the antibody specific for the human GLUT-3 epitope tag could not be visualized.

Discussion

In this study, our goal was to characterize the role of two major GLUT-4 targeting motifs in insulin-sensitive cells. Epitope-tagged GLUT-4 constructs, in which mutations were made at either the phenylalanine residue at position 5 (FAG) or the leucine residues at positions 489–490 (LAG), were stably expressed in 3T3-L1 adipocytes. FAG accumulated at the plasma membrane in the absence of insulin, irrespective of its expression level, whereas LAG accumulated at the plasma membrane only when the mutant was overexpressed at levels that were fourfold endogenous GLUT-4 levels. Despite these defects in basal targeting, an insulin-dependent movement out of the intracellular fraction was still evident for both LAG and FAG suggesting that neither the FQVI nor the LL motifs play a direct role in the insulin-regulated movement of GLUT-4 to the plasma membrane. These results suggest that both the NH₂- and COOH-terminal targeting motifs play important yet functionally distinct roles in GLUT-4 targeting in adipocytes.

The strategy employed in this study was designed to address some of the potential conflicts that have arisen from previous GLUT-4 targeting studies (reviewed in James and Piper, 1994). We have employed a stable expression plasmid, pMex, to express our constructs in 3T3-L1 cells (Benito et al., 1991). This cell line provides a useful model for these studies as it is possible to obtain stable transfectants that differentiate into highly insulin-responsive adipocytes. The pMex vector achieves a level of expression that approximates endogenous GLUT-4 levels expressed in 3T3-L1 adipocytes (Fig. 3). Such considerations are important, as one of the major variables between previous GLUT-4 targeting studies was the level of expression obtained for recombinant transporters due to the use of different expression systems (Asano et al., 1992; Piper et al., 1992; Czech et al., 1993; Verhey et al., 1993). This may be critical as it has been shown that the overexpression of endosomal/TGR proteins may saturate intracellular retention mechanisms in mammalian cells and thus severely complicate the interpretation of results (Wong and Hong, 1993; Reaves and Banting, 1994). We have analyzed the targeting of recombinant proteins in several stably transfected clonal adipocytes to examine the effects of different expression levels (Fig. 3). Furthermore, we utilized two

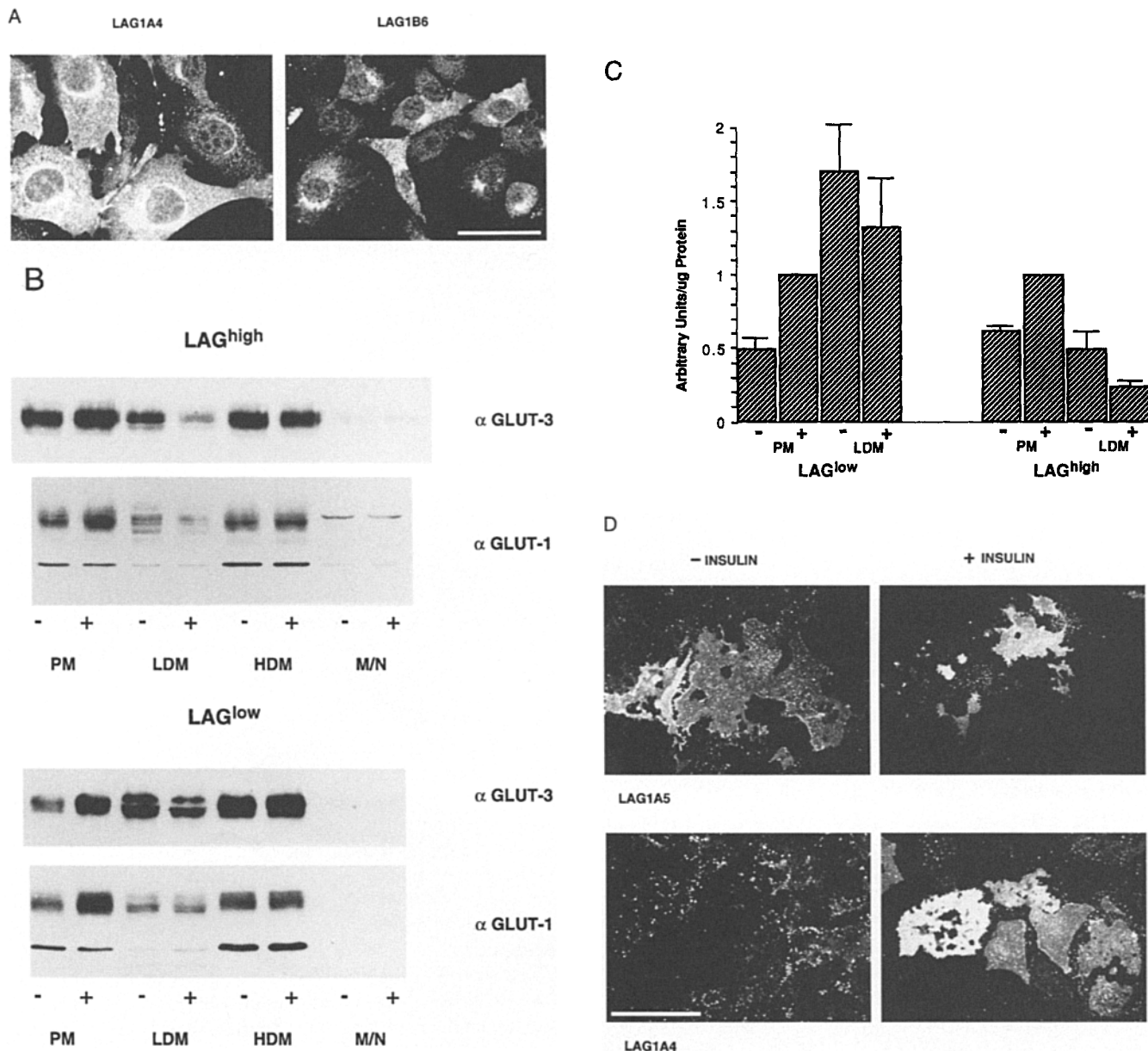


Figure 6. Localization of LAG in stably-transfected 3T3-L1 cells. (A) Immunolocalization of LAG constructs in stably-transfected 3T3-L1 fibroblasts by confocal immunofluorescence microscopy. Cells were fixed, permeabilized, and labeled with an antibody specific for the COOH terminus of GLUT-4 (R820) and FITC-conjugated sheep anti-rabbit antibody. Shown are fibroblast clones LAG1A4 (left) and LAG1B6 (right). Images were collected, adjusted for brightness and contrast and printed using identical conditions. (B–D) Subcellular distribution of epitope-tagged recombinant GLUT-4 (LAG) expressed at low (LAG1D3, LAG1B6, LAG1A4) or high (LAG1A5) levels in basal (–) and insulin-stimulated (+) 3T3-L1 adipocytes. (B) Subcellular membrane fractions (10 μ g) prepared by differential centrifugation were subjected to SDS-PAGE, electrophoretically transferred to nitrocellulose membranes and immunoblotted with either an affinity-purified antibody specific for the human GLUT-3 epitope tag (R1697, top) or an antibody specific for the COOH terminus of GLUT-1 (R493, bottom). Signals were detected by ECL. (C) The combined results of multiple independent differential centrifugation experiments were quantitated by densitometry and plotted for basal (–) and insulin-stimulated (+) adipocytes. Values are the means \pm SEM (arbitrary units/ μ g protein). (D) Immunofluorescence labeling of PM lawns prepared from LAG-transfected 3T3-L1 adipocytes incubated in the absence (left) or presence (right) of insulin for 15 min at 37°C. Plasma membrane fragments prepared from LAG-transfected adipocytes were immunolabeled with the human GLUT-3 antibody. Shown are adipocyte clones LAG1A5 (top) and LAG1A4 (bottom). Bars: (A and D) 50 μ m.

separate subcellular fractionation schemes, that are well established for these cells, and which enable unambiguous analysis of glucose transporter targeting. This was fundamental to these studies since the primary method used to assess GLUT-4 targeting by a variety of groups has been immunofluorescence microscopy (Czech et al., 1993; Ver-

hey et al., 1993; Corvera et al., 1994). Immunofluorescence localization of our constructs in stably-transfected 3T3-L1 fibroblasts failed to clearly resolve the intracellular distribution of these recombinant proteins (Figs. 2 A, 5 A, and 6 A). As noted by others previously, this technique is prone to artifact; similar ambiguous results have been attributed

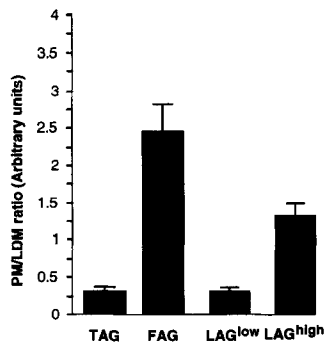


Figure 7. The PM/LDM ratios of recombinant transporter constructs in basal adipocytes were calculated from data obtained for all individual clones over multiple separate experiments. Data from experiments with either TAG or FAG-transfected 3T3-L1 adipocyte clones were pooled and considered as representative of a phenotype distribution for TAG or FAG respectively, due to the

consistency of results for individual clones irrespective of their levels of expression. TAG values were calculated from 10 separate determinations for clones TAG3B1 and TAG2D5. The results of five separate determinations for clones FAG1D1, FAG3C2 and FAG2C5 are shown for FAG. Values presented as the LAG^{low} phenotype were calculated from six separate determinations for clones LAG1D3 and LAG1B6. LAG^{high} values were calculated from four separate determinations for clone LAG1A5. Values are shown as the means \pm SEM for a minimum of four independent determinations.

to both differences in expression levels and to inadequate resolution using this technique (Asano et al., 1992; Hudson et al., 1992; Griffiths et al., 1993; Verhey et al., 1993). The use of a nondisruptive epitope tag was preferred to undertaking a chimeric approach, as recombinant chimeras may alter conformational determinants essential to proper GLUT-4 targeting. Our results indicate that the targeting of epitope-tagged GLUT-4 (TAG) over a wide range of expression levels was indistinguishable from that of wild-type GLUT-4, as reported here and in previous studies (Calderhead et al., 1990; Holman et al., 1990; Piper et al., 1991; Robinson and James, 1992). Similar results were obtained in several different clones expressing TAG at levels approximately two- to sixfold greater than endogenous GLUT-4 (Fig. 2).

Our assessment of the subcellular distribution of recombinant GLUT-4 transporters clearly shows that both the NH₂-terminal phenylalanine and COOH-terminal dileucine motifs function in the targeting of GLUT-4 in 3T3-L1 adipocytes. Mutation of either of these motifs to alanine resulted in a marked accumulation of recombinant GLUT-4 at the cell surface in an insulin-independent manner. This resulted in impaired insulin action by default because the index of this phenomenon involves accumulation of the protein at the plasma membrane. However, both FAG (F⁵ to A) and LAG (L⁴⁸⁹L⁴⁹⁰ to AA) retained their insulin-dependent movement out of the intracellular LDM vesicle fraction suggesting that neither of these motifs directly regulates the insulin-dependent translocation of GLUT-4 per se. Hence, we propose that the information that encodes the insulin regulatability of GLUT-4 must be located elsewhere in the protein.

The observation that LAG accumulated at the cell surface only when overexpressed, whereas FAG accumulated at the cell surface irrespective of expression level, suggests that these two domains may regulate distinct targeting events. The fact that the LL mutant had a wild-type subcellular distribution at low expression suggests that under these conditions other targeting motifs must compensate

for this mutation. This could include either the NH₂-terminal FQQI motif or other motifs elsewhere in the protein. Alternatively, the dileucine residues may comprise only part of a larger motif, in which case mutation of these residues to alanine might not greatly disrupt its overall tertiary structure. It is important to note that the dileucine signal is flanked by the phosphorylation site in GLUT-4 (Lawrence et al., 1990), and it will be of interest to determine if mutation of L⁴⁸⁹L⁴⁹⁰ to AA abrogates phosphorylation of the transporter in an expression-dependent manner. It has been postulated previously that the relative affinities of aromatic- and dileucine-based motifs for either internalization or intracellular sorting functions could be altered either by phosphorylation-dephosphorylation, or by other posttranslational modifications (reviewed in Trowbridge et al., 1993). That FAG exhibited a high cell surface distribution irrespective of its expression level suggests that other motifs were unable to compensate for this defect. This implies that this motif may be intimately involved in regulating the movement of GLUT-4 between the cell surface and endosomes or vice versa.

The dependence of LAG targeting upon expression level may account for our inability to detect a role for the GLUT-4 carboxy terminus on intracellular targeting in the past (Piper et al., 1992, 1993). Previously, we have used Sindbis virus to express chimeras comprised of portions of GLUT-1 and GLUT-4 in CHO cells. Only chimeras containing the NH₂ terminus of GLUT-4 targeted in a manner similar to GLUT-4. These results are consistent with the present studies given a moderate level of expression of the chimeric constructs. However, it remains unclear why other groups have been unable to demonstrate an effect of the NH₂ terminus on GLUT-4 targeting, particularly since we have observed this effect in a variety of different cell lines and using different modes of cDNA expression.

What is the function of these targeting domains in the intracellular trafficking of GLUT-4? While we have not specifically addressed this question in the present studies, it is possible to speculate based on previous work. It is known, largely from EM studies, that GLUT-4 recycles between the cell surface and intracellular tubules and vesicles via the classical coated pit/endosomal pathway (Slot et al., 1991a,b; Robinson et al., 1992). In the absence of insulin, GLUT-4 appears to be withdrawn from this recycling system (Slot et al., 1991b) and this is consistent with the fact that GLUT-4 is actively retained within the cell (Holman et al., 1990). The nature of the intracellular compartment in which GLUT-4 is stored is poorly defined but it is thought to be somewhat specialized (reviewed in Birnbaum, 1992 and James and Piper, 1994), and so the targeting of GLUT-4 to this compartment may confer its unique insulin regulation. The NH₂- and COOH-terminal GLUT-4 targeting motifs were first identified by studying the distribution of GLUT-1/GLUT-4 chimeras in fibroblasts (Piper et al., 1992; Czech et al., 1993; Marshall et al., 1993; Verhey et al., 1993). From these studies it was shown that when added to GLUT-1 either the NH₂ or COOH terminus of GLUT-4 could, to a certain extent, recapitulate the unique intracellular sequestration of the entire GLUT-4 protein. Both of these motifs have been reasonably well characterized in fibroblasts and CHO cells and have been shown to have the capacity to regulate internalization

(Corvera et al., 1994; Garippa et al., 1994). Garippa et al. (1994) demonstrated that the amino terminus of GLUT-4, when substituted for the transferrin receptor cytoplasmic domain, functions to promote the efficient internalization of the protein from the cell surface in a manner critically dependent upon the residue at position 5. In addition, mutation of F⁵ to A caused a marked reduction in GLUT-4 targeting to cell surface clathrin-coated pits in CHO cells (Piper et al., 1993). Furthermore, these motifs resemble motifs found in many other endosomal proteins. Thus, it is tempting to conclude that the predominant role of these domains is to regulate GLUT-4 internalization. While these domains may play a role in GLUT-4 internalization, kinetic analysis of different transporters in 3T3-L1 adipocytes indicate that there is not a significant difference in the internalization rates between GLUT-1 and GLUT-4 (Yang and Holman, 1993). Thus, this suggests that these motifs must regulate additional functions in the intracellular sorting of GLUT-4. This most likely involves either the retention of GLUT-4 in endosomes or its sorting into the specialized compartment that is withdrawn from the endosomal system. Consistent with this type of model, it has been shown that aromatic residue-based motifs and dileucine motifs play distinct though functionally similar roles in other proteins. For instance, the cytoplasmic tail of the cation-independent mannose 6-phosphate/IGF II receptor (CI-MPR) contains an aromatic residue-based motif (YKYSKV) that primarily regulates internalization but contributes additionally, although not significantly, to intracellular Golgi sorting, and a dileucine based motif adjacent to the aromatic motif that regulates cycling between the Golgi and late endosomes (Johnson and Kornfeld, 1992). Disruption of the aromatic-based motif critically disrupts internalization of the receptor resulting in its accumulation at the cell surface, whilst having only a slight effect upon intracellular sorting (Lobel et al., 1989; Johnson and Kornfeld, 1992). Conversely, mutation of the dileucine residues abrogates intracellular sorting without altering internalization of the receptor (Johnson and Kornfeld, 1992).

Defects in GLUT-4 translocation are likely to occur in insulin-resistant disease states such as non-insulin-dependent diabetes mellitus (NIDDM). The basis for such defects remain unknown, but patients with NIDDM have been found to have levels of GLUT-4 similar to those of normal individuals (Kahn, 1992). We have shown that the phenylalanine-based NH₂-terminal and the COOH-terminal dileucine motifs play important and distinct roles in GLUT-4 targeting in the insulin-responsive 3T3-L1 adipocyte cell line. These findings may help lead to the identification of the protein machinery that facilitates GLUT-4 translocation and thus yield major insights into insulin action. Further studies of the molecular regulation of GLUT-4 targeting are thus essential to elucidate the precise mechanisms by which the amino and carboxy-terminal motifs function to regulate the targeting of GLUT-4. Unravelling the exact nature of these regulatory processes may provide a useful model with which to study a number of other important proteins that recycle between the plasma membrane and intracellular loci, and to determine the extent to which signalling sequences may be conserved between such proteins.

We gratefully acknowledge Dr. A. Carozzi, Dr. W. Pascoe, and B. Sullivan for their invaluable technical support. We thank C. Macqueen for technical assistance with fluorescence and confocal microscopy, R. Wilson for the transmembrane topology diagram of GLUT-4, and Dr. J. Slot, Dr. D. Hume, and Dr. J. Stow for their helpful discussions during the course of this study. We also thank S. Rea, Dr. Rob Piper, Dr. D. Pulford and Dr. D. Hume for their critical reading of the manuscript.

This work was supported by a National Health and Medical Research Council grant. D. E. James is a recipient of a Wellcome Trust Senior Research Fellowship.

Received for publication 9 May 1995 and in revised form 9 June 1995.

References

- Alm, R. A., and J. S. Mattick. 1995. Identification of a gene, *pilV*, required for type 4 fimbrial biogenesis in *Pseudomonas aeruginosa*, whose product possesses a pre-pilin-like leader sequence. *Mol. Microbiol.* 16:485-496.
- Asano, T., K. Takata, H. Katagiri, K. Tsukuda, J. Lin, H. Ishihara, K. Inukai, H. Hirano, Y. Yazaki, and Y. Oka. 1992. Domains responsible for the differential targeting of glucose transporter isoforms. *J. Biol. Chem.* 267:19636-19641.
- Balch, W. E., W. G. Dunphy, W. A. Braell, and J. E. Rothman. 1984. Reconstruction of the transport of protein between successive compartments of the Golgi measured by the coupled incorporation of N-acetylglucosamine. *Cell.* 39:405-416.
- Bell, G., T. Kayano, J. Buse, C. Burant, J. Takeda, D. Lin, H. Fukumoto, and S. Seino. 1990. Molecular biology of mammalian glucose transporters. *Diabetes Care.* 13:198-206.
- Benito, M., A. Porras, A. R. Nebreda, and E. Santos. 1991. Differentiation of 3T3-L1 fibroblasts to adipocytes induced by transfection of *ras* oncogenes. *Science (Wash. DC).* 253:565-568.
- Birnbaum, M. J. 1989. Identification of a novel gene encoding an insulin-responsive glucose transporter protein. *Cell.* 57:305-315.
- Birnbaum, M. J. 1992. The insulin-responsive glucose transporter. *Int. Rev. Cytol.* 137A:239-297.
- Blok, J., E. M. Gibbs, G. E. Lienhard, J. W. Slot, and H. J. Geuze. 1988. Insulin-induced translocation of glucose transporters from post-Golgi compartments to the plasma membrane of 3T3-L1 adipocytes. *J. Cell Biol.* 106:69-76.
- Calderhead, D., K. Kitagawa, L. Tanner, G. Holman, and G. Lienhard. 1990. Insulin regulation of the two glucose transporters in 3T3-L1 adipocytes. *J. Biol. Chem.* 265:13800-13808.
- Charron, M. J., F. C. I. Brosius, S. L. Alper, and H. F. Lodish. 1989. A glucose transport protein expressed predominantly in insulin-responsive tissues. *Proc. Natl. Acad. Sci. USA.* 86:2535-2539.
- Corvera, S., A. Chawla, R. Chakrabarti, M. Joly, J. Buxton, and M. P. Czech. 1994. A double leucine within the GLUT4 glucose transporter COOH-terminal domain functions as an endocytosis signal. *J. Cell Biol.* 126:979-989.
- Cushman, S. W., and L. J. Wardzala. 1980. Potential mechanism of insulin action on glucose transport in the isolated rat adipose cell. *J. Biol. Chem.* 255:4758-4762.
- Czech, M. P., A. Chawla, C. Woon, J. Buxton, M. Armoni, W. Tang, M. Joly, and S. Corvera. 1993. Exofacial epitope-tagged glucose transporter chimeras reveal COOH-terminal sequences governing cellular location. *J. Cell Biol.* 123:127-135.
- Fukumoto, H., T. Kayano, J. B. Buse, Y. Edwards, P. F. Pilch, G. Bell, and S. Seino. 1989. Cloning and characterization of the major insulin-responsive glucose transporter expressed in human skeletal muscle and other insulin-responsive tissues. *J. Biol. Chem.* 264:7776-7779.
- Garippa, R. J., T. W. Judge, D. E. James, and T. E. McGraw. 1994. The amino terminus of GLUT4 functions as an internalization motif but not an intracellular retention signal when substituted for the transferrin receptor cytoplasmic domain. *J. Cell Biol.* 124:705-716.
- Gould, G. W., V. Derechin, D. E. James, K. Tordjman, S. Ahern, E. M. Gibbs, G. E. Lienhard, and M. Mueckler. 1989. Insulin-stimulated translocation of the HepG2/erythrocyte type glucose transporter expressed in 3T3-L1 adipocytes. *J. Biol. Chem.* 264:2180-2184.
- Griffiths, G., R. G. Parton, J. Lucoq, B. Van Deurs, D. Brown, J. W. Slot, and H. J. Geuze. 1993. The immunofluorescent era of membrane traffic. *Trends Cell Biol.* 3:214-219.
- Haney, P. M., J. W. Slot, R. C. Piper, D. E. James, and M. Mueckler. 1991. Intracellular targeting of the insulin-regulatable glucose transporter (GLUT4) is isoform specific and independent of cell type. *J. Cell Biol.* 114:689-699.
- Harris, D. S., J. W. Slot, H. J. Geuze, and D. E. James. 1992. Polarized distribution of glucose transporter isoforms in Caco-2 cells. *Proc. Natl. Acad. Sci. USA.* 89:7556-7560.
- Holman, G. D., I. J. Kozka, A. E. Clark, C. J. Flower, J. Saltis, A. D. Habberfield, I. A. Simpson, and S. W. Cushman. 1990. Cell surface labeling of glucose transporter isoform GLUT4 by bis-mannose photolabel. *J. Biol. Chem.* 265:18172-18179.
- Hudson, A. W., M. Ruiz, and M. J. Birnbaum. 1992. Isoform-specific subcellular targeting of glucose transporters in mouse fibroblasts. *J. Cell Biol.* 116:

- 785–797.
- James, D. E., and R. C. Piper. 1994. Insulin resistance, diabetes, and the insulin-regulated trafficking of GLUT-4. *J. Cell Biol.* 126:1123–1126.
- James, D. E., R. Brown, J. Navarro, and P. F. Pilch. 1988. Insulin-regulatable tissues express a unique insulin sensitive glucose transport protein. *Nature (Lond.)* 333:183–185.
- James, D. E., M. Strube, and M. Mueckler. 1989. Molecular cloning and characterization of an insulin regulatable glucose transporter. *Nature (Lond.)* 338:83–87.
- James, D. E., R. C. Piper, and J. W. Slot. 1993. Targeting of mammalian glucose transporters. *J. Cell. Science.* 104:607–612.
- Johnson, K. F., and S. Kornfeld. 1992. The cytoplasmic tail of the mannose 6-phosphate/insulin-like growth factor-II receptor has two signals for lysosomal enzyme sorting in the Golgi. *J. Cell Biol.* 119:249–257.
- Kahn, B. B. 1992. Facilitative glucose transporters: regulatory mechanisms and dysregulation in diabetes. *J. Clin. Invest.* 89:1367–1374.
- Lawrence, J. C., J. F. Hiken, and D. E. James. 1990. Phosphorylation of the glucose transporter in rat adipocytes. *J. Biol. Chem.* 265:2324–2332.
- Lobel, P., K. Fujimoto, R. D. Ye, G. Griffiths, and S. Kornfeld. 1989. Mutations in the cytoplasmic domain of the 275 kd mannose 6-phosphate receptor differentially alter lysosomal enzyme sorting and endocytosis. *Cell.* 57:787–796.
- Marshall, B. A., H. Murata, R. C. Hresko, and M. Mueckler. 1993. Domains that confer intracellular sequestration of the GLUT-4 glucose transporter in *Xenopus* oocytes. *J. Biol. Chem.* 268:26193–26199.
- Piper, R. C., L. J. Hess, and D. E. James. 1991. Differential sorting of two glucose transporters expressed in insulin-sensitive cells. *Am. J. Physiol.* 260:C570–C580.
- Piper, R. C., C. Tai, J. W. Slot, C. S. Hahn, C. Rice, H. Huang, and D. E. James. 1992. The efficient intracellular sequestration of the insulin-regulatable glucose transporter (GLUT4) is conferred by the NH₂ terminus. *J. Cell Biol.* 117:729–743.
- Piper, R. C., C. Tai, P. Kulesza, S. Pang, D. Warnock, J. Baenziger, J. W. Slot, H. J. Geuze, C. Puri, and D. E. James. 1993. GLUT-4 NH₂ terminus contains a phenylalanine-based targeting motif that regulates intracellular sequestration. *J. Cell Biol.* 121:1221–1232.
- Reaves, B., and G. Banting. 1994. Overexpression of TGN38/41 leads to mislocalisation of gamma-adaptin. *FEBS Lett.* 351:448–456.
- Robinson, L. J., and D. E. James. 1992. Insulin-regulated sorting of glucose transporters in 3T3-L1 adipocytes. *Am. J. Physiol.* 263:E383–E393.
- Robinson, L. J., S. Pang, D. S. Harris, J. Heuser, and D. E. James. 1992. Translocation of the glucose transporter (GLUT4) to the cell surface in permeabilized 3T3-L1 adipocytes: effects of ATP, insulin, and GTPγS and localization of GLUT4 to clathrin lattices. *J. Cell Biol.* 117:1181–1196.
- Simpson, I. A., D. R. Yver, P. J. Hissin, L. J. Wardzala, E. Karnieli, L. B. Salans, and S. W. Cushman. 1983. Insulin-stimulated translocation of glucose transporters in the isolated rat adipose cells: characterization of subcellular fractions. *Biochem. Biophys. Acta.* 763:393–407.
- Slot, J. W., H. J. Geuze, S. Gigengack, D. E. James, and G. E. Lienhard. 1991a. Translocation of the glucose transporter GLUT4 in cardiac myocytes of the rat. *Proc. Natl. Acad. Sci. USA.* 88:7815–7819.
- Slot, J. W., H. J. Geuze, S. Gigengack, G. E. Lienhard, and D. E. James. 1991b. Immunolocalization of the insulin regulatable glucose transporter in brown adipose tissue of the rat. *J. Cell Biol.* 113:123–135.
- Suzuki, K., and T. Kono. 1980. Evidence that insulin causes the translocation of glucose transport activity to the plasma membrane from an intracellular storage site. *Proc. Natl. Acad. Sci. USA.* 77:2542–2545.
- Trowbridge, I. S., J. F. Collawn, and C. R. Hopkins. 1993. Signal-dependent membrane protein trafficking in the endocytic pathway. *Annu. Rev. Cell Biol.* 9:129–161.
- Verhey, K. J., and M. J. Birnbaum. 1994. A Leu-Leu sequence is essential for COOH-terminal targeting signal of GLUT4 glucose transporter in fibroblasts. *J. Biol. Chem.* 269:2353–2356.
- Verhey, K. J., S. F. Hausdorff, and M. J. Birnbaum. 1993. Identification of the carboxy terminus as important for the isoform-specific subcellular targeting of glucose transporter proteins. *J. Cell Biol.* 123:137–147.
- Wong, S. H., and W. Hong. 1993. The SXYQRL sequence in the cytoplasmic domain of TGN38 plays a major role in trans-Golgi network localization. *J. Biol. Chem.* 268:22853–22862.
- Yang, J., and G. D. Holman. 1993. Comparison of GLUT4 and GLUT1 subcellular trafficking in basal and insulin-stimulated 3T3-L1 cells. *J. Biol. Chem.* 268:4600–4603.